JOURNAL OF MATERIALS SCIENCE 20 (1985) 895–905

Isotactic polypropylene/polyisobutylene blends: morphology–structure–mechanical properties relationships

L. BIANCHI, S. CIMMINO, A. FORTE, R. GRECO, E. MARTUSCELLI *, F. RIVA, C. SILVESTRE
Istituto di Ricerche su Tecnologia dei Polimeri e Reologia del CNR, Via Toiano 6, 80072 Arco Felice, Napoli, Italy

Morphological observations by optical and scanning electron microscopy, wide (WAXS) and small (SAXS) angle X-ray scattering, differential scanning calorimetry (DSC) and mechanical tests have been performed on sheet specimens of isotactic polypropylene (iPP)/polyisobutylene (PIB) blends obtained under different crystallization conditions. Two kinds of morphologies have been observed, particularly at high crystallization temperature T_c, on thin sections of the same sheets: a spherulitic one in the centre and a row-like structure on the edges. The size of the spherulites, as well as the thickness of the row-like regions, decreases with diminishing T_c, and seems to be independent of the amount of rubber. The adhesion among the spherulites and between the spherulites and the row-like regions seems to become poorer with higher T_c. The rubber particles seem to be evenly dispersed into the iPP matrix for samples quenched at low temperatures, whereas for samples isothermally crystallized (at high T_c) their concentration seems to be slightly higher at the border of the spherulites than in the centre. The overall crystallinity measured by DSC and by WAXS is an increasing function of T_c and decreases with increasing amount of PIB. The β index of iPP phase, quite low indeed (max $\simeq$ 3%), drops with lowering T_c and with enhancing PIB percentage. The long spacing L for a given quenching temperature T_q is independent of PIB content, whereas for isothermally crystallized samples at low undercooling varies differently according to T_c. The lamellar thickness L_c is always a decreasing function of rubber content. Stress–strain analysis shows a more and more brittle behaviour both with increasing T_q (beyond $T_c = 122^\circ$ C all the specimens are very brittle irrespective of PIB amount) and PIB amount in accordance with the morphological observations. Some tentative hypotheses have been made to explain the observed behaviour.

1. Introduction

It is well known that isotactic polypropylene (iPP) shows a low impact resistance at temperatures close to or below room temperature. Such a shortcoming is due to its relatively high glass transition temperature (-10°C). In recent years people in industry have designed a series of suitable blend formulations by adding at least one rubbery component to the iPP matrix. Of course most of such compounds were made on a purely empirical knowledge. Therefore only a very poor scientific understanding of their behaviour, and particularly of the mechanisms responsible for their impact performance improvements, has been achieved. On this basis in our Institute a few years ago a series of investigations [1, 2] were undertaken on some similar systems: the examined ternary blends consisted of iPP, high density polyethylene (HDPE)

*To whom all correspondance should be addressed.

0022–2461/85 $03.00 + .12

and ethylene-propylene random rubbery copolymer (EPM). Such systems showing good impact at performance, however, were too complex to allow a complete understanding of their structure–properties relationships. Therefore a systematic study on simpler binary blends was successively undertaken. The aim was to investigate the influence of a rubbery component, polyisobutylene (PIB), ethylene–propylene random copolymers (EPM), ethylene–propylene–diene terpolymers (EPDM), with different molecular mass and structure) on the morphology, thermal and crystallization behaviour of thin films of iPP, isothermally crystallized, at low undercoolings.

The results showed that nucleation, radial growth of spherulites and overall crystallization processes as well as dimensions and structure of lamellar and interlamellar regions are greatly dependent upon blend composition and nature of rubbery component [3, 4].

It was found moreover that dispersed rubber domains (pre-existing or formed during the crystallization of iPP phase) are ejected, occluded and deformed by the growing spherulites. Such processes, that require energy, may be responsible in the case of many of the above mentioned effects [5, 6]. In the present paper we report results of a further study on iPP/PIB blends, started recently [7], in which samples much thicker ($\simeq 1$ mm) than in the previous case, crystallized at different degrees of undercooling, have been used. Moreover on the same specimens morphological observations by optical and scanning electron microscopy, wide angle (WAXS) and small angle (SAXS) X-ray scattering as well as macroscopic tensile mechanical tests have been performed.

The influence of a rubbery component (PIB) on: (i) the overall morphology of blend samples; (ii) the dimensions and structure of lamellar and interlamellar regions; (iii) the polymorphism of iPP; (iv) the primary nucleation process; (v) the tensile mechanical properties has been investigated. The main aim was to find suitable correlations between crystallization conditions, blend composition, structural and morphological parameters and mechanical properties.

2. Experimental details

2.1. Materials

Isotactic polypropylene (iPP) ($\bar{M}_w = 3.1 \times 10^5$ and $\bar{M}_n = 1.6 \times 10^4$) was kindly provided by RAPRA. Polyisobutylene was a commercial sample (Vistanex LM-MH produced by Esso with $\bar{M}_v = 6.6 \times 10^4$).

2.2. Blend preparation

Blends of isotactic polypropylene (IPP) and a polyisobutylene (PIB) rubber containing 0, 10, 20, 30% by weight of PIB were prepared by melt mixing in a Brabender-like apparatus (Haake Rheocord).

The material so obtained, sandwiched between two teflon sheets, was hot-pressed in a common hydraulic press (Wabash) at 200° C and 200 kg cm^{-2}. Then the pressure was released and the sandwich was suddenly immersed in a thermostated bath (kept at a prefixed temperature within ± 0.4° C). In such way sheet samples 0.5 and 1.25 mm thick were: (a) isothermally crystallized (IC) at various temperatures, T_c (from 122 to 132° C), and (b) non isothermally crystallized (NIC) at different T_q (25; 60 and 90° C) between two Teflon surfaces.

2.3. Mechanical tensile test

Dumb-bell specimens were cut from the above mentioned sheets and elongated by an Instron machine (at room temperature and at a constant crosshead speed of 10 mm min^{-1}). From the stress–strain curves so obtained two parameters were calculated: (a) the Young modulus from the initial slope $[d\sigma/d\epsilon]_{\epsilon=0}$ and (b) the strength σ_r from the breakage point. It is to be noted that part of the samples ruptured before yield or during the cold drawing whereas the rest of them broke after complete fibre formation.

2.4. Morphology

The overall morphology of the blends was investigated by optical and scanning electron microscopy. Optical micrographs were taken by using a Leitz Ultraphot microscope on sections of the sample (obtained by means of an Ultratome LKB). Scanning electron microscopy was carried out by using a Philips 501 B SEM on cryogenically fractured samples.

The number of spherulites per unit area was counted on an average of three sections of microtomed specimens, for a semiquantitative analysis.

2.5. WAXS measurements

Wide angle X-ray scattering (WAXS) measurements were carried out by a (PW 1050 Model) Philips

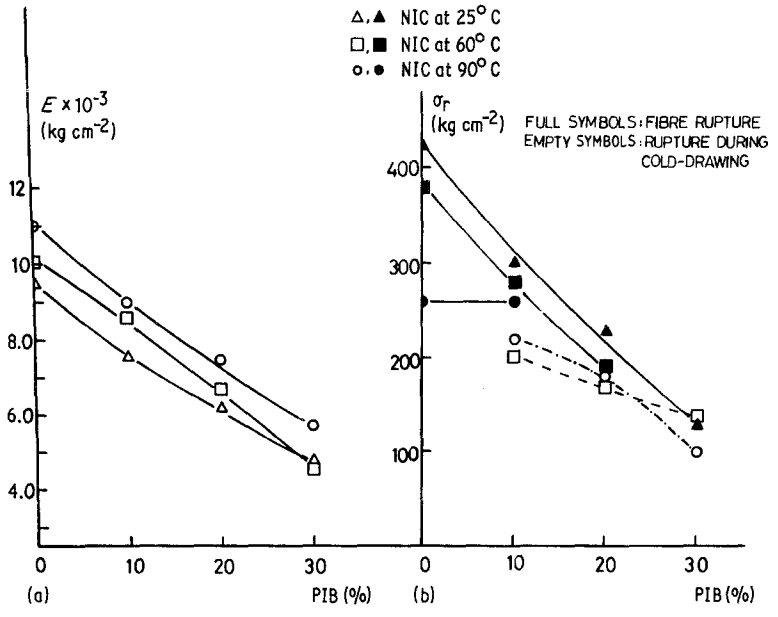

Figure 1 Modulus E and strength σ_r as a function of PIB percentage for specimens non isothermally crystallized (NIC) at temperatures: 25° C (triangles), 60° C (squares) and 90° C (circles). Empty symbols: specimens ruptured during cold-drawing; full ones: specimens ruptured after complete fibre formation.

powder diffractometer (Cu$K\alpha$ nickel-filtered radiation) to evaluate (a) the crystallinity, following the Hermans–Weidinger method [8], and (b) the content of β form of iPP, according to Turner-Jones [9].

The crystallinity index, x_c, of the blends was corrected, using a simulation program elaborated by us [10], to evaluate the erroneous intensity increase of the (1 1 0) iPP reflection (due to the superimposition of the PIB amorphous halo).

2.6. SAXS measurements

Small angle X-ray scattering (SAXS) spectra (Cu$K\alpha$ nickel-filtered radiation) were collected by a step by step automatized Rigaku Denki camera with a resolving power up to about 80 nm, scanning 2θ angle at intervals of 0.02°; counting times were 1000 seconds per point. The intensities were corrected: (a) for the parasitic scattering (background); (b) for absorption; (c) for the slit smearing, by using the Schmidt method [11].

3. Results and discussion

3.1. Mechanical tensile properties

The modulus and the strength of nonisothermally crystallized specimens (NIC) are reported as a function of PIB percentage in Fig. 1. The modulus decreases almost linearly with increasing PIB content. Moreover it diminishes also with decreasing quenching temperature (T_q). Both the findings can be mostly attributed to a decrease of the overall crystallinity content (as shown in Figs. 6 and 7 elsewhere).

The strength behaviour is more complex since, depending on T_q and on the percentage of PIB, the specimens rupture: (a) after fibre formation (full symbols) and (b) before (empty ones). In fact at 25° C all the specimens are very ductile undergoing fibre rupture after neck formation and propagation (cold drawing); at 60° C pure iPP undergoes fibre rupture whereas the blend specimens containing 30% of PIB all break before yield. Between these two extreme behaviours the blend specimens containing 10 and 20% of PIB rupture partly after complete fibre formation and partly before, at 90° C an analogous behaviour is shown, but in this case already at 20% of PIB content the fibre is not formed any more. Such findings are better shown in Table I, where the fraction of samples fractured

TABLE I Fraction, y, of specimens fractured as fibres as a function of quenching temperature T_q and PIB content in the blends

T_q (° C)	PIB (wt %)			
	0	10	20	30
25	1	1	1	1
60	1	0.5	0.2	0
90	1	0.4	0	0

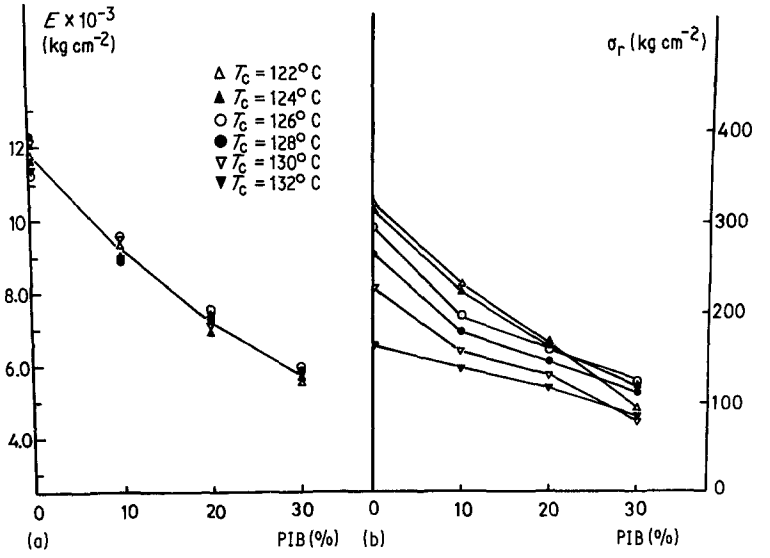

Figure 2 Modulus E and strength σ_r as a function of PIB percentage for specimens isothermally crystallized (IC) at different temperatures as indicated.

as fibres, y, is reported as a function of T_q and PIB content (%).

A progressive embrittlement of the blends in dependence of an increase of T_q as well as of PIB amount is observed. The y values are only qualitative as no accurate statistical analysis could be made on the basis of the few specimens used (seven on average). The modulus as well as the strength of samples isothermally crystallized at temperature from 122 up to 132° C are reported in Fig. 2. The modulus decreases with increasing percentage of PIB and it seems to be, in the limit of experimental error, almost independent of the crystallization temperature. Both the results can be attributed to the overall crystallinity content of the blends, which diminishes of course with increasing rubber content, whereas it stays almost constant with temperature in the considered range (122 to 132° C).

The strength of the specimens, i.e. all that undergo a brittle failure before yield, decreases with increasing PIB content. Furthermore, particularly at low PIB content, the strength shows a lowering with augmentation of the crystallization temperature, T_c. At higher PIB content such an effect is lower and all the curves tend to merge together.

The very brittle behaviour of the IC samples and the more ductile one of the NIC specimens, at constant PIB content, can be attributed to the different number of tie-molecules [12–14] trapped among the iPP crystallites at different undercoolings. In fact, as soon as the material undergoes a very rapid quenching (i.e. at 60° C and even at 25° C) the crystallization can occur only locally. Only a scarce possibility is given to the longer chains to disentangle from each other because of their low mobility. Therefore a considerable amount of entangled molecules, present in the melt [15], will act as tie-molecules among the crystallites after sample crystallization. This effect renders the material very highly interconnected. Furthermore the quenched specimens show low lamellae thickness (see Fig. 9) and low crystal perfection. All these features make the material very ductile and therefore capable of yield.

In contrast when crystallization is carried out at higher temperatures (i.e. IC samples), the polymer molecules are able to disentangle and to orderly adhere to the crystallite substrates; hence only a few tie-chains, capable of carrying the load, are available. In addition more perfect and thick crystalline lamellae will develop offering a higher resistance to slipping and fragmentation. Since such processes occur during necking initiation and propagation the specimens fracture more and more easily in a brittle manner the higher T_c or T_q. Increasing the PIB content at constant T_c or T_q the number per unit volume of rubber particles occluded in intraspherulitic regions increases in the system. This renders the cold-flow of the iPP

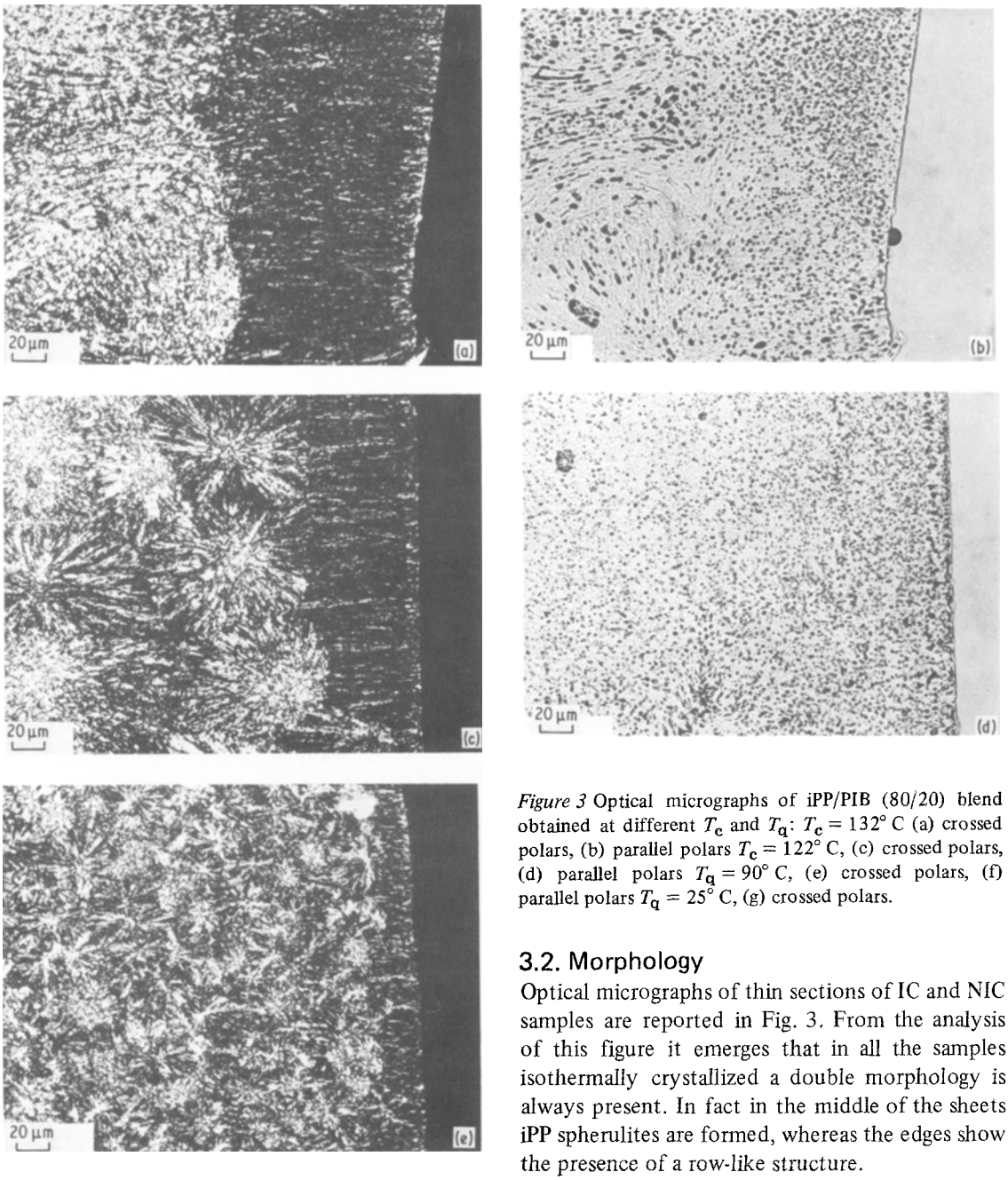

Figure 3 Optical micrographs of iPP/PIB (80/20) blend obtained at different T_c and T_q: $T_c = 132°$ C (a) crossed polars, (b) parallel polars $T_c = 122°$ C, (c) crossed polars, (d) parallel polars $T_q = 90°$ C, (e) crossed polars, (f) parallel polars $T_q = 25°$ C, (g) crossed polars.

matrix more and more difficult and induces a higher and higher instability with rupture that, starting locally (where highest is the stress concentration), will produce more and more a brittle fracture the greater is the amount of PIB.

Therefore the y values reported in Table I depend both on T_q and on the PIB content (note that in the upper left-hand side corner y is equal to unity and in the lower right-hand side corner the y value is zero).

3.2. Morphology

Optical micrographs of thin sections of IC and NIC samples are reported in Fig. 3. From the analysis of this figure it emerges that in all the samples isothermally crystallized a double morphology is always present. In fact in the middle of the sheets iPP spherulites are formed, whereas the edges show the presence of a row-like structure.

The row-like morphology results from a higher concentration of aligned nuclei on the sample–Teflon contact surface. Such nuclei can either be formed during the crystallization or pre-exist. It is not clear at present what the cause of this phenomenon is. One possibility is the fact that cavities or rough surfaces often are able to catalyse the formation of crystallization nuclei. On the other hand it is also possible that, during the fusion, the nuclei have not been completely destroyed and migrate toward the surface because

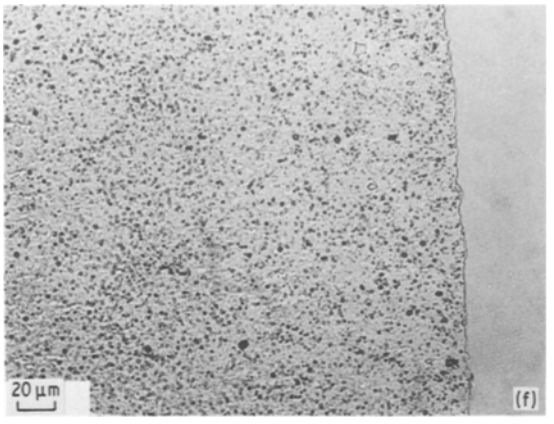

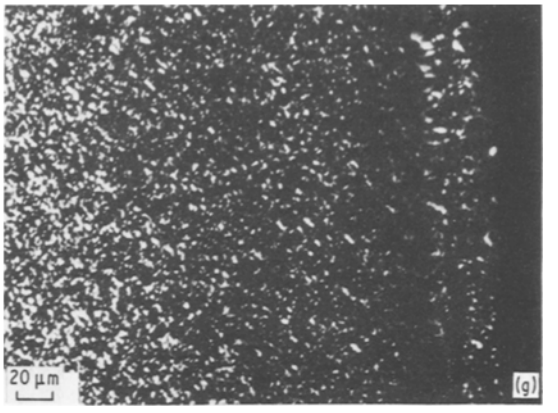

Figure 3 continued.

of the particular rheological patterns existing in the melt before crystallization.

The presence of row-like structures is, moreover, usually observed when a polymeric material is crystallized on cold surfaces. In this case such a phenomenon has been attributed to the effect of a thermal gradient [12–13, 16]. For IC samples the percentage of the material that crystallizes according to a row-like morphology increases with increasing T_c (see Figs. 3a and c), namely 25% and 40% for $T_c = 122$ and 132° C, respectively, (see Table II), and it seems not to be influenced by the rubber content.

For NIC samples the presence of a row-like morphology depends on the crystallization conditions: in fact for the samples obtained at 25° C no row-structures were observed (see Fig. 3g) whereas in the case of the samples obtained at 60 and 90° C (see Fig. 3c) the fraction of material with the row-like morphology increased gradually with T_q. The dimensions of iPP spherulites for the IC specimens depended on T_c and sample thickness. The number of spherulites per unit area (N/S) in fact increased with decreasing T_c and, for the same T_c, with decreasing sample thickness, as reported in Table III.

No nucleation effect was produced on iPP by PIB addition since N/S did not vary significantly with rubber content.

Different results were observed by Martuscelli *et al.* [4] analysing the morphology of thin films of iPP/PIB blends obtained by means of the following different procedure: (a) the two polymers, previously purified, were dissolved, in the desired proportions, in xylene at 120° C; (b) the solvent was rapidly evaporated and (c) the blend powders were compression moulded to give thin films. It was found that the elastomer worked

TABLE II Percentage of material that crystallizes according to a row-like morphology as function of T_c and thickness, t, of the sheet samples

T_c(° C)	iPP/PIB	Row structure (%)	
		t = 0.5 mm	t = 1.25 mm
132	100/0	39 ± 2	20 ± 1
	90/10	42 ± 2	21 ± 1
	80/20	36 ± 1	20 ± 1
	70/30	37 ± 2	27 ± 1
126	100/0	26 ± 1	19 ± 1
	90/10	27 ± 2	17 ± 1
	80/20	20 ± 2	15 ± 2
	70/30	23 ± 3	15 ± 1
122	100/0	21 ± 2	17 ± 1
	80/20	22 ± 1	14 ± 1
	70/30	21 ± 1	15 ± 1

TABLE III Number of spherulites per 1 mm² of area (N/S) as function of T_c and sheet sample thickness, t, for IC blend

T_c(° C)	iPP/PIB	Number of spherulites (N/S)	
		t = 0.5 mm	t = 1.25 mm
132	100/0	76 ± 7	54 ± 3
	90/10	58 ± 6	27 ± 3
	80/20	62 ± 1	42 ± 3
	70/30	73 ± 6	42 ± 5
126	100/0	92 ± 2	66 ± 5
	90/10	98 ± 2	50 ± 2
	80/20	114 ± 5	48 ± 8
	70/30	101 ± 9	69 ± 4
122	100/0	146 ± 8	74 ± 1
	80/20	142 ± 8	83 ± 4
	70/30	153 ± 4	97 ± 2

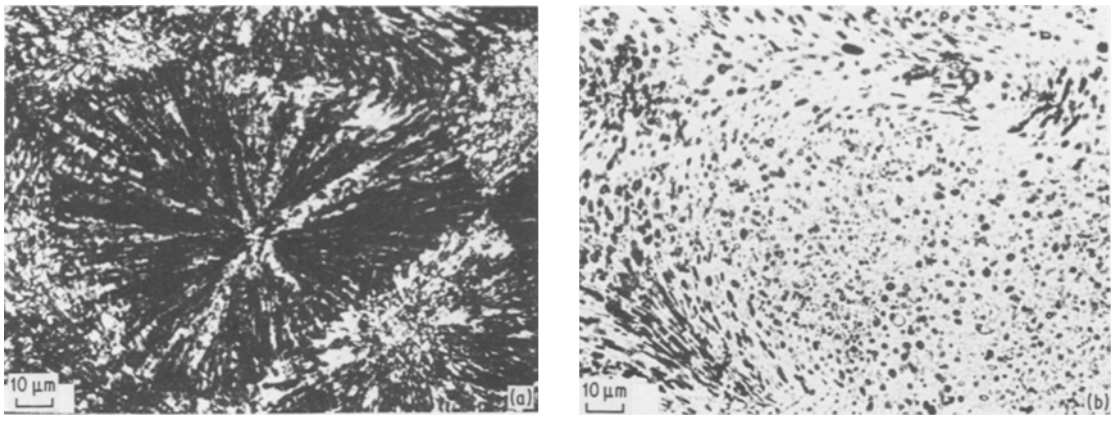

Figure 4 Optical micrographs of iPP/PIB (80/20) blend crystallized at $T_c = 122°$ C (a) crossed polars and (b) parallel polars.

as an effective nucleating agent. In particular the values of the number of spherulites per unit area were also 30 times higher than that relative to pure iPP (namely for iPP/PIB 90/10 blend at $T_c = 135°$ C). Such results seem to be in disagreement with those reported in the present paper. This disagreement probably may be attributed to the different conditions of sample preparation and thickness, to the fact that the starting polymers used in the present work were not purified and also to the fact that the temperature of precrystallization (i.e. the temperature at which the samples were kept before being brought to T_c) was not the same. In particular with regard to the latter, it must be mentioned that such a temperature strongly determines the presence or the absence of pre-existing nuclei and their amount.

The particles of the disperse phase, for the IC samples, are often aligned along a concentric ring at the border of the spherulite (Figs. 3a and b, and 4a and b). Such a phenomenon may be explained assuming that during the crystallization the domains of the disperse phase are rejected for a short distance. Then they are occluded in the spherulitic regions and deformed in two different ways: by the spherulitic growing front and by the squeezing action that neighbouring spherulites, just before impingement, have on the melt phase, which consist mostly of rejected amorphous iPP chains and PIB particles. Therefore they are preferentially located at the borders of spherulites even though they are occluded in the central core as well (see Fig. 4). This explanation is in good agreement with the theory of Omenyi and coworkers [19–21] modified by Bartczak and some of us [5], that described the rejection, engulfing and/or deformation of amorphous domains by a crystallizable polymeric front that grows according to a spherulitic morphology when the rate of crystallization is not very high. In the case of NIC samples the domains of the PIB, of droplet-like shape, are distributed homogeneously on all the sample (Figs. 3e and f, and 5a and b). In this case, the rate of crystallization becomes so high that the

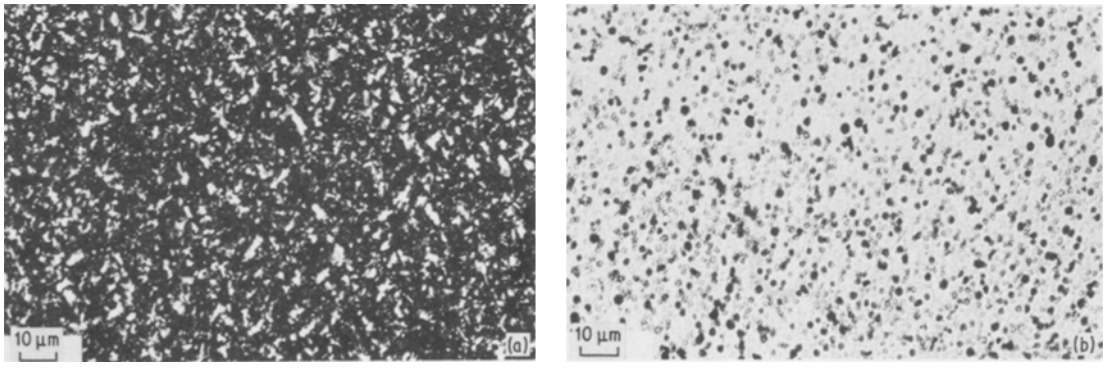

Figure 5 Optical micrographs of iPP/PIB (80/20) blend crystallized at $T_q = 60°$ C (a) crossed polars, and (b) parallel polars.

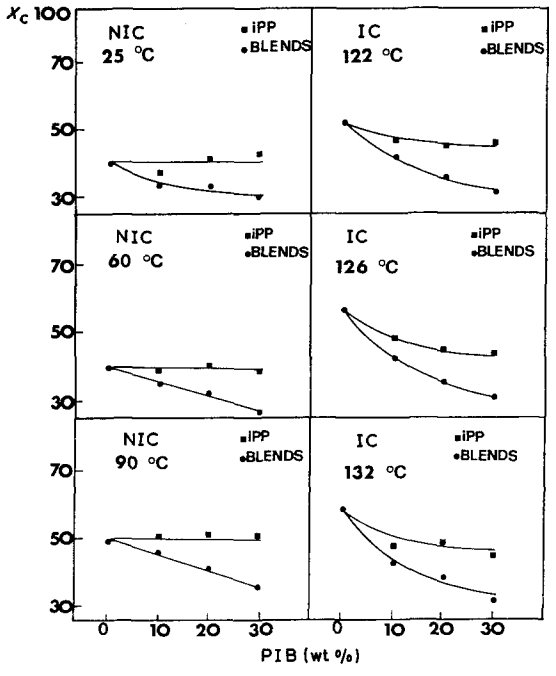

Figure 6 Crystallinity index, x_c, by DSC, of the blends and of the iPP phase as a function of elastomer content and temperature as indicated.

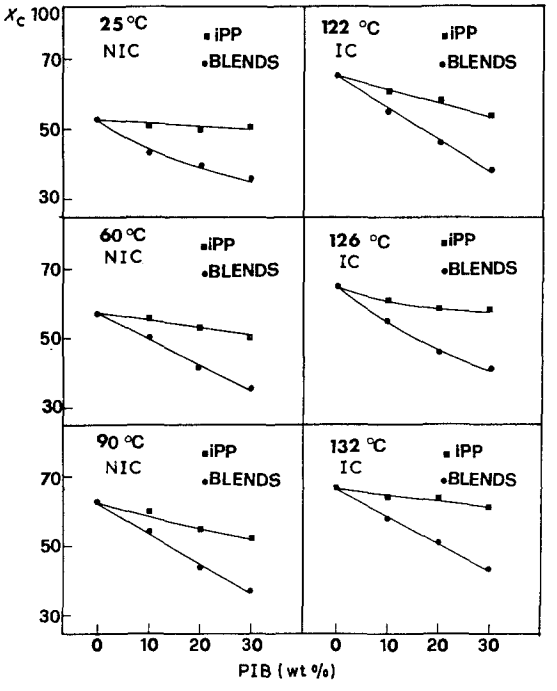

Figure 7 Crystallinity index, x_c, by WAXS, of the blends and of the iPP phase as a function of elastomer content and temperature as indicated.

PIB particles remain suddenly occluded in the matrix with a low possibility of being rejected.

3.3. Structural analysis

The overall x_c of the blends and the x_c referred to for the iPP phase, obtained by DSC and WAXS, are reported in Figs. 6 and 7 for different crystallization conditions, as a function of the elastomer percentage. As shown, the x_c values of the iPP phase, especially for isothermally crystallized blends, seem to decrease with increasing PIB content. Such an observation indicates that the presence of the rubber may influence the perfection of the growing iPP crystals and/or reduce the portion of the crystallizable polymer. WAXS analysis on α and β form content shows that in the samples isothermally crystallized at higher temperature the index of β form is relatively low ($\simeq 3\%$) and is drastically lowered by the addition of PIB (see Fig. 8). The β index is also dependent upon the crystallization conditions. In blends crystallized non isothermally at 25 and 60° C no β form is detectable.

3.4. Superreticular parameters

The desmeared SAXS profiles (Fig. 9) show well defined maxima whose intensity decreases with increasing rubber content. From such maxima the long spacing L was derived by applying the Bragg law. A too strong interference effect in all the examined SAXS profiles did not allow to apply the well-known Hosemann–Joerchel method [22, 23] to obtain the average crystalline particle dimensions. Assuming for the spherulite fibrillae a two phase model then, from L values, the crystalline lamella thickness, L_c, can be calculated by using the relation:

$$L_c = \frac{x_c L}{(\rho_c/\rho_a)(1-x_c)+x_c}$$

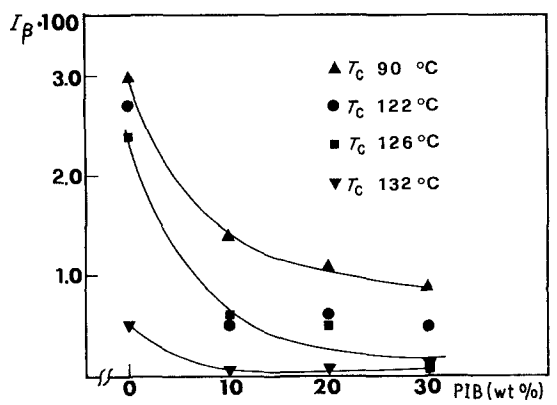

Figure 8 β form index, I_β, of iPP–PIB blends as a function of rubber content and temperature as indicated.

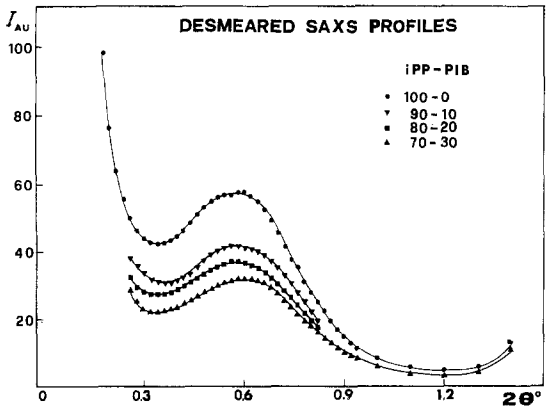

Figure 9 Desmeared SAXS profiles of iPP–PIB blends non isothermally crystallized at 60° C.

where x_c is the WAXS crystallinity index of iPP, ρ_c and ρ_a are the densities of the crystalline and amorphous iPP phases, respectively. The dependence of the long spacing L and of the lamella thickness L_c on PIB content, for a given crystallization condition, is shown in Figs. 10 and 11, respectively.

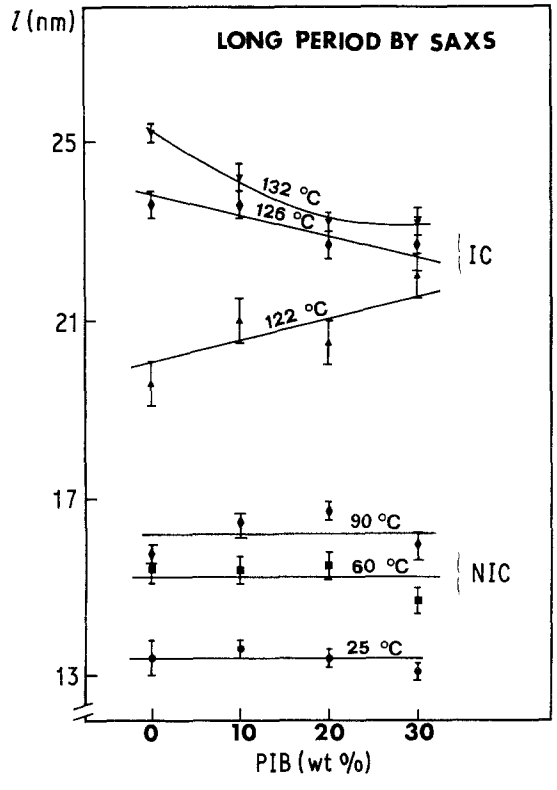

Figure 10 Long period, L, of iPP–PIB blends, by SAXS, as a function of elastomer content and temperature as indicated.

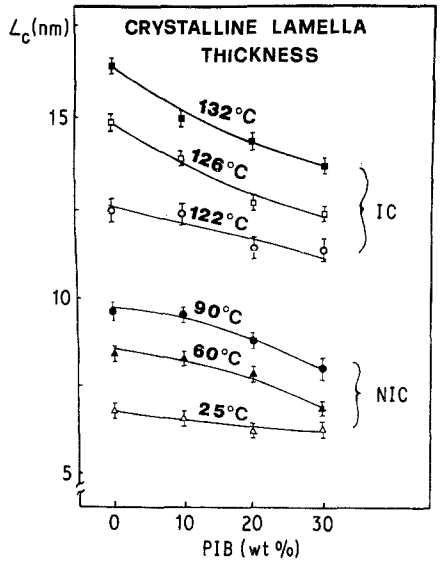

Figure 11 Crystalline lamella thickness, L_c, of iPP–PIB blends as a function of elastomer content and temperature as indicated.

It can be observed that L in case of NIC samples is almost independent of blend composition. For samples isothermally crystallized at high T_c (126 and 132° C) L decreases with increasing the concentration of PIB; an opposite trend is shown by samples crystallized at 122° C. For a given blend, L always increases with T_c.

The lamella thickness monotonically diminishes, for a given crystallization condition, with enhancing the elastomer content. Thus when iPP crystallizes from its blends in the presence of the PIB, lamella crystals are formed whose thickness (measured along a direction that is almost coincident with the chain axis) is lower the higher the PIB content becomes. Such a behaviour cannot be explained simply by thermodynamical considerations. In fact, if the PIB acted in the melt as iPP diluent (i.e. if the polymers were compatible) one should expect, at a given crystallization temperature, an increase of L_c with increasing rubber concentration, because of the corresponding undercooling lowering, even tough variations of the surface free energy of folding cannot be predicted *a priori* [24].

It is likely that morphological and kinetic, rather than thermodynamic, effects are responsible for the L_c depression: the inclusion of spherical elastomer domains in intraspherulitic regions during iPP spherulite growth may in fact cause some kind of hindrance to the lamellar crystal development.

4. General discussion and summary

The results above discussed separately, accordingly to the various techniques of investigations, can be summarized as follows.

4.1. Effect of the crystallization conditions on the blend properties

When the material is suddenly quenched at low T_q (25° C) from the molten state it crystallizes at a very high rate. The chain conformations typical of the melt are mostly frozen and only local crystallization can occur. The material exhibits a low crystallinity content (see DSC results in Figs. 6 and 7) and very thin lamellae (as shown in Fig. 11), since very little possibility is given for their development. Moreover the quenching does not allow sufficient time for nuclei alignment and hence no row-like morphology can be observed. The net result is a very homogeneous and highly interconnected material with a high ductility and an easy fibre formation. In fact the elevated number of tie-molecules, coupled with the intrinsic weakness of the thin crystallites, favours the crystal fragmentation necessary to their reorientation in the necking zone for fibre formation.

At very high T_c (i.e. at all IC temperatures) the crystallization rate decreases strongly and the system tends to approach real thermodynamic conditions of crystallization. In fact much longer times are given to the chains to make them disentangle from each other, therefore, more regular chain folding and more perfect crystals can be achieved. The crystallinity content is quite high (Figs. 6 and 7) and the crystallite lamellae thickness as well (Fig. 11). The consequence is a brittle behaviour due to the low number of tie-molecules necessary to carry the load as well as to the high resistance to fragmentation offered by the thicker and better crystallites. Such findings are in close analogy with those of Brown and Ward [25] for pure polyethylene. With respect to the rubbery phase the particles are partly rejected during the crystallization by the advancing front of the growing spherulites and are also squeezed in the intraspherulitic regions at the moment where the spherulites start to impinge upon each other. Therefore the particle density is lower in intraspherulitic regions than outside. Moreover some coalescence phenomena during the rejection tend to increase their size and the squeezing action to elongate them along some circular path (see Fig. 4). The adhesion between the spherulitic and row-like regions and among the spherulites is very poor in the case of IC samples (Figs. 12 and 13) and seems to increase for NIC blends. This effect, which is also confirmed by mechanical tests, is due to the increasing number of chains connecting crystallites and spherulites as soon as the crystallization rate is increased.

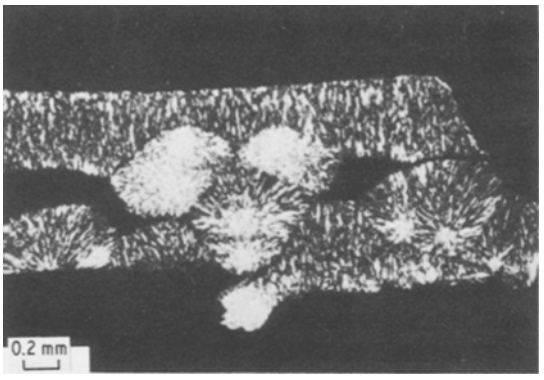

Figure 12 Optical micrograph of iPP/PIB (80/20) blend crystallized at T_c = 132° C (crossed polars).

Some semibrittle behaviour can be observed, as discussed in a previous section of this paper, in the case of NIC samples quenched at higher temperatures (T_q = 60 and 90° C) than 25° C.

4.2. Effect of the rubber phase content on the iPP matrix

At constant T_c or T_q an increase of PIB content decreases the overall crystallinity and therefore the Young's modulus. Furthermore, since no adhesion exists between the rubber particles and the iPP matrix, it is only the latter which carries all the external load. Hence also the brittleness and the strength decrease with increasing PIB percentage.

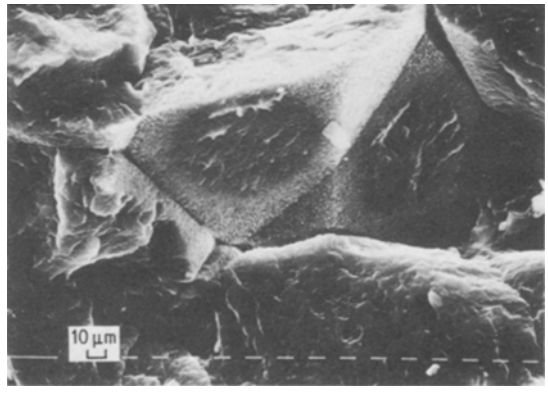

Figure 13 Scanning electron micrograph of iPP/PIB (90/10) blend crystallized at T_c = 126° C.

For NIC samples, for which the long spacing L is constant, the decrease in L_c with PIB% results in amorphous regions, that is the distance between the crystallites. This can induce in some way, as a possible secondary effect, a diminution of the number of tie-molecules connecting the crystallites and can worsen, as a consequence, the mechanical behaviour.

Summarizing, the embrittlement effect (increasing T_c or T_q) is due to the reduction of the interconnecting tie-molecules as well as to the thickening and to the perfection improvements of the lamellae. The increase of PIB content reduces more and more the cross-section of the matrix, which, in the absence of adhesion between rubber particles and matrix (as from the morphological observations it seems to be the case), carries all the load. Concluding this paper, it is to be noted that the results, discussed above, are to be considered preliminary since work is still in progress to investigate the effect of varying PIB molecular mass on the structure, morphology and mechanical properties of the iPP matrix.

Acknowledgement

This work was partly supported by "Progetto Finalizzato Chimica Fine e Secondaria" del CNR.

References

1. L. D'ORAZIO, R. GRECO, C. MANCARELLA, E. MARTUSCELLI and G. RAGOSTA, *Polym. Eng. Sci.* **22** (1982) 536.
2. L. D'ORAZIO, R. GRECO, E. MARTUSCELLI and G. RAGOSTA, *ibid.* **23** (1983) 489.
3. E. MARTUSCELLI, C. SILVESTRE and G. ABATE, *Polymer* **23** (1982) 229.
4. E. MARTUSCELLI, C. SILVESTRE and L. BIANCHI, *ibid.* **24** (1983) 1458.
5. Z. BARTCZAK, A. GALESKI and E. MARTUSCELLI, *Polym. Eng. Sci.* in press.
6. A. GALESKI, E. MARTUSCELLI and M. PRACELLA, *J. Polym. Sci. Phys. Ed.* **22** (1984) 739.
7. L. BIANCHI, A. BUONANNO, A. FORTE, R. GRECO, MA RONG TANG, E. MARTUSCELLI, F. RIVA and C. SILVESTRE, VI Conférence Européenne des Plastiques, Paris, June 1982, p. IV-20.
8. P. H. HERMANS and A. WEIDINGER, *Makromol. Chem.* **50** (1961) 98.
9. A. TURNER-JONES, J. M. AIZELWOOD and D. R. BECKETT, *ibid.* **75** (1964) 134.
10. E. MARTUSCELLI, F. RIVA, A. FORTE and A. BUONANNO, to be published.
11. P. W. SCHMIDT, *Acta Crystallogr.* **19** (1965) 938.
12. A. PETERLIN, *Polym. Eng. Sci.* 17 (1977) 183.
13. *Idem, ibid.* **18** (1968) 1062.
14. *Idem, ibid.* **19** (1979) 118.
15. J. D. FERRY, Proc. 5th Int. Congr. Rheol., 1 (1969) 3.
16. M. I. KOHAN "Nylon Plastics" (John Wiley and Sons, New York, 1973) pp. 291–99.
17. E. S. CLARK, in "Polymeric Materials", (American Chemical Society for Metals, 1975) pp. 1–54.
18. S. S. KATTI and J. M. SCHULTZ, *Polym. Eng. Sci.* **22** (1982) 1001.
19. S. N. OMENYI, A. W. NEUMANN, W. W. MARTIN, G. M. LESPINARD and R. P. SMITH, *J. Appl. Phys.* **52** (1981) 789.
20. S. N. OMENYI, A. W. NEUMANN and O. J. VAN OSS, *ibid.* **52** (1981) 796.
21. S. N. OMENYI and A. W. NEUMANN, *ibid.* **47** (1976) 3956.
22. R. HOSEMANN and S. N. BAGCHI, "Direct Analysis of Diffraction by Matter" (North Holland, Amsterdam, 1962).
23. F. RIVA and A. FORTE, Preprints of the International Rubber Conference 82, Paris, June 1982, pp. 1–25.
24. E. MARTUSCELLI, *Polym. Eng. Sci.* in print.
25. N. BROWN and I. M. WARD, *J. Mater. Sci.* **18** (1983) 1405.

Received 6 January
and accepted 30 April 1984